



# Florida Onsite Sewage Nitrogen Reduction Strategies Study

Task D.13

**Validate/Refine Aquifer-Complex Soil Model**

**White Paper**

May 2015

442-27-001

**HAZEN AND SAWYER**  
Environmental Engineers & Scientists

In association with:



**AET**  
Applied Environmental Technology

**Otis Environmental  
Consultants, LLC**

# **Florida Onsite Sewage Nitrogen Reduction Strategies Study**

## **TASK D.13 WHITE PAPER**

### **VALIDATE/REFINE AQUIFER-COMPLEX SOIL MODEL**

#### **Prepared for:**

Florida Department of Health  
Division of Disease Control and Health Protection  
Bureau of Environmental Health  
Onsite Sewage Programs  
4042 Bald Cypress Way Bin #A-08  
Tallahassee, FL 32399-1713

FDOH Contract CORCL

**May 2015**

#### **Prepared by:**

**HAZEN AND SAWYER**  
Environmental Engineers & Scientists

In Association With:







## Section 1.0

### Introduction

---

As part of Task D for the Florida Onsite Sewage Nitrogen Reduction Strategies (FOSNRS) Study a combined vadose zone and saturated zone model is being developed and refined (STUMOD-FL-HPS). This report, prepared by the Colorado School of Mines (CSM), documents work completed on Task D.13, Validate/Refine Aquifer-Complex Soil Model with Data Collected from Task C. FOSNRS Task D.13 involves revising and improving the aquifer model, validation of the integrated aquifer and complex soil model, and corroboration of the revised model to field data as available (including Task C Home Sites).

The aquifer model (horizontal plane source, HPS, also referred to as the saturated zone module) is coupled with STUMOD-FL to obtain boundary concentrations for the saturated zone for nitrogen species infiltrating through the soil treatment unit to the water table. Concentration reaching the water table is the only parameter calculated by STUMOD-FL that is used in the saturated zone module. However, the saturated zone module may also be run independently of STUMOD-FL with user provided values for contaminant concentrations at the water table. Thus it was determined that more valuable information would be obtained by doing validation independently on the saturated zone module. See the FOSNRS Task D.10 report for validation and refinement of STUMOD-FL.

The combined model, STUMOD-FL-HPS was corroborated to FOSNRS Task C data collected at a home site (CHS-2) and the University of Florida Gulf Coast Research and Education Center (GCREC) Soil and Groundwater (S&GW) Test Facility (TA1).



## Section 2.0

### Validation of the Aquifer Model

---

The first step is validating the model theory and tool itself by comparisons with other methods and models. For this step, a comparison to a numerical model that is based on principle of conservation of mass was used to check the validity of the HPS model itself. The traditional idea of validation is to assure that the model can make accurate and reproducible predictions outside the period of time over which it was calibrated. Other approaches to validation originated from the idea that verifying the model performance by simply comparing outputs and observations under conditions outside of calibration does not assure that the model is correct. This suggests that traditional validation may not allow sufficient insight to decide if the model structure and parameterization are consistent with the physics of the simulated processes. Furthermore, the approach of comparing simulated outputs and observations that were not used for model calibration may not be a good approach when the quality and quantity of the observations used for comparison with model outputs are not sufficient to allow an adequate validation. Thus, other approaches have been introduced as a validation process. Vogel and Sankarasubramanian (2003) used a validation approach that focuses on the ability of the hypothesized model structure to represent the observed covariance structure of the input and output time series without even calibrating the model. In this work, we use a comparison to a numerical model that is based on principle of conservation of mass to check the validity of the STUMOD-FL-HPS model. To further validate our model using the traditional approach of comparing simulated outputs to observations outside of calibration conditions, we calibrated the model using the data collected from the surficial aquifer at the GCREC mound (see FOSNRSTask D.12 report).

The validation/refinement procedure involves checking the veracity of the model and refining the model using field data. A comparison between results obtained from the HPS solution to those from a numerical model for a non-decaying synthetic contaminant has been completed as validation of the mathematics, solution scheme, and implementation of the solution scheme in Excel VBA used to derive and solve the HPS solution (Tonsberg, 2014). The numerical models that were used were MODFLOW and MT3DMS (Harbaugh, 2005; Zheng and Wang, 1999). Comparison to numerical models was done to provide supporting evidence as to the utility of this tool for evaluating contaminant transport from an onsite wastewater treatment system (OWTS) in aquifers. Two

simulations using the numerical models were carried out for comparison to the HPS solution. The first simulation considers a homogeneous one dimensional velocity field, while the other considers a heterogeneous one dimensional velocity field; the HPS solution was derived to consider the latter. The first comparison establishes the mathematical soundness of the HPS solution while the second comparison examines potential limitations of the HPS solution for a specific case.

## 2.1 The One Dimensional Homogenous Velocity Case

A numerical model (MODFLOW/MT3DMS) was created using 161 columns, 624 rows and 21 layers. The finite difference grid was refined along the portion of the model where concentration was monitored. The grid spacing for this area was 1.25 meters by 0.625 meters by 0.625 meters in the 'X', 'Y' and 'Z' directions, respectively. The total dimensions of the finite difference grid were 50 meters deep by 2172 meters wide by 780 meters long. These dimensions are intended to represent an aquifer of infinite areal extent and of finite thickness. Dispersivity values assigned were 5 meters in the longitudinal direction and 2.5 meters in the transverse horizontal and vertical directions. The dispersivity values ensured that the grid Peclet number is less than one. The grid Peclet number is a measure of the degree to which the transport problem is dominated by advection. It is critical for understanding potential error introduced by the numerical solution schemes (Zheng and Bennett, 2002). The hydraulic conductivity was 120 m/yr and a porosity/specific yield of 0.3 was assigned to the entire domain. "Constant Flux" boundary conditions were used for the upper and lower boundaries of the model and "No Flow" boundaries were assigned along the lateral extent of the model. The constant flux across each cell at the upper and lower extent of the finite difference grid was calculated using Darcy's approach (equation 2-1) such that the seepage velocity was constant, at 10 m/yr. This was later verified by examining the cell-by-cell flow file produced by MODFLOW.

$$v_x = \frac{q}{n} = -\frac{K_{sat}}{n} \frac{dh}{dl} \quad (2-1)$$

A contaminant source was created to replicate a horizontal plane 2.5 by 3 meters with a HLR of 1 m/yr. The concentration of the synthetic contaminant in the recharge water was 32 mg/l, no decay was considered. The total mass flux of contaminant to the aquifer was 240 g/yr. Forty monitoring wells were placed along the centerline of the expected plume at the surface of the finite difference grid and at 1, 3, 5, and 9 meters below the surface. The wells were located from 20 to 755 meters from the contaminant source plane. The simulation was run at steady state conditions.

While the numerical model requires a finite difference grid and complex algorithms to accurately solve the governing equations the HPS solution does not. The same conceptual model used to build the numerical model was also used to construct an HPS simulation. The contaminant transport problems considered by the HPS solution and the numerical model were identical in every way except the manner in which they were solved. The HPS solution was used to calculate contaminant concentrations at the same locations within the hypothetical aquifer. Because the HPS solution does not consider volumetric flux, a mass flux of 240 g/yr was applied at the contaminant source plane. The dimensions of the source plane, porosity, seepage velocity and dispersivity values were identical to those that were used in the MODFLOW/MT3DMS model. The results from this comparison are presented in Figures 2.1 and 2.2, which indicate that the HPS solution accurately calculates the contaminant concentration at all locations. This comparison is a validation of the mathematical derivation of the HPS solution. These results also validate the numerical integration technique that is used to solve equation 3-2 in Task D.11, and to ensure that the implementation of the solution in excel VBA was correct. While the trapezoidal integration technique can introduce error for functions that change rapidly the HPS solution is relatively constant under steady state conditions and thus the integration technique is appropriate.

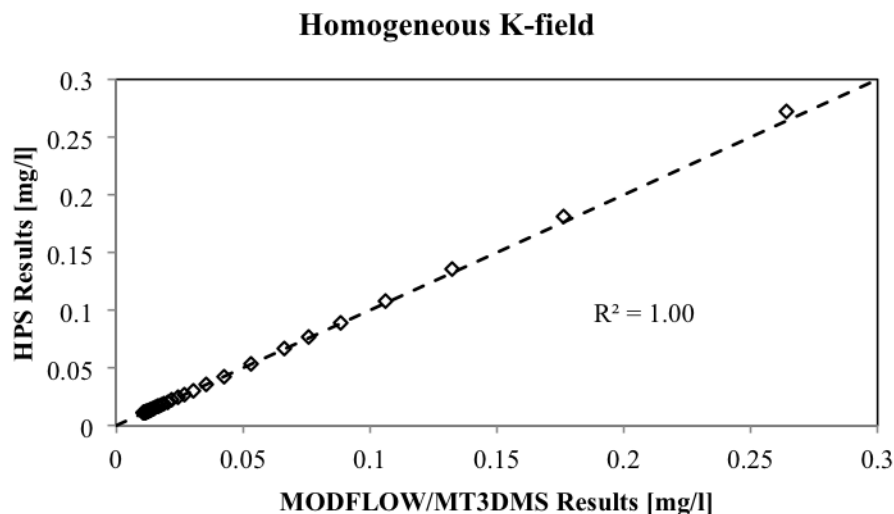


**Figure 2.1**  
**Validation results for the HPS solution indicate that it will accurately calculate concentration for a homogeneous velocity, one dimensional advection and three dimensional dispersion transport problem.**

## 2.2 The One Dimensional Heterogeneous Velocity Case

A one dimensional homogeneous velocity is not likely to occur within an actual aquifer due to heterogeneities in hydraulic conductivity, variable recharge, and anthropogenic activity such as extraction wells. The question that is likely to arise is whether the HPS solution can be successfully applied in situations where these ideal conditions do not exist. It would be difficult to quantify all the possible errors that may be incurred by applying the HPS solution to situations where a one dimensional advection field does not exist. However, one specific case is presented here where the HPS solution was compared to results from a numerical model with a heterogeneous velocity field in one dimension (Figure 2.2).

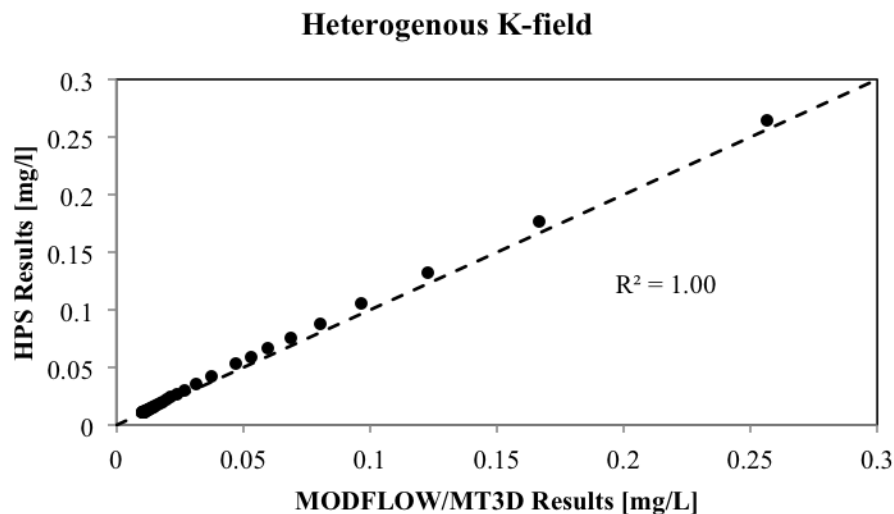


**Figure 2.2**  
Results from a comparison of the HPS solution to a numerical model with a one dimensional heterogeneous velocity field.

The numerical model presented in Section 2.1 was used as a base to build a new numerical model with a heterogeneous velocity field. The same parameter values were used to construct this model with one difference. The hydraulic conductivity field was constructed using a random number generator. The hydraulic conductivity field of the new model possessed the same mean hydraulic conductivity as did the previous model. The hydraulic conductivity values that were generated were drawn from a log normal distribution and ranged over three orders of magnitude. The resultant seepage velocities within the finite difference cells varied from 0 – 4387 m/yr but maintained a mean velocity of 10 m/yr, which was verified in the cell-by-cell flow file produced by MODFLOW. Be-

cause of this a direct comparison to the HPS solution was possible. Descriptive statistics for the hydraulic conductivity field as well as the calculated seepage velocity for this set-up are found in Tables 2.1 and 2.2.

**Table 2.1**  
**Descriptive Statistics of the Heterogeneous Hydraulic Field used in the Numerical Model to Validate the HPS Solution.**

Hydraulic Conductivity [m/yr]	
Mean	119.97
Median	84.84
Mode	44.96
Standard Deviation	119.95
Range	7331.05
Minimum	1.44
Maximum	7332.49
Count	2109744

**Table 2.2**  
**Descriptive Statistics of the Resultant Velocity Field Produced by the Random Hydraulic Conductivity Field.**

Seepage Velocity [m/yr]	
Mean	10.1
Median	9.0
Mode	0
Standard Deviation	10.1
Range	4387.1
Minimum	0
Maximum	4387.1
Count	2109744

Concentrations calculated by the HPS solution presented in FOSNRS Task D.11 were also used for comparison to the results from the numerical model with a heterogeneous hydraulic conductivity field. Because the mean velocity remained the same for the heterogeneous hydraulic conductivity numerical model, it may be expected that no possible differences could exist in the results. However, the working hypothesis was that two possible phenomenon could occur which would result in differences between the HPS solution and the heterogeneous hydraulic conductivity numerical model. The first condition is that increased longitudinal and transverse dispersion due to local differences in velocity could occur. The result from this would be decreased concentrations at the ob-



servation points in the heterogeneous model. Results in Figure 2.2 would not fall along the one-to-one line and the RMS error displayed in Figure 2.3 would be larger than the homogeneous case. The second phenomenon that could have occurred would have been transverse advection instead of purely longitudinal advection. This could occur if adjacent cells had higher hydraulic conductivities than the cells immediately down gradient. This arrangement of hydraulic conductivity might promote advective movement around cells of lower hydraulic conductivity.

Results from the numerical model indicate that heterogeneities in velocity do not have a significant impact and that the HPS solution is still valid under these conditions (Figures 2.2 and 2.3). The results are important because they show that velocity heterogeneities do not have a substantial impact so long as they do not cause preferential flow or transverse advection to occur. In regards to the working hypothesis, local variations in velocity do not appear to increase dispersion in any dimension under steady state conditions. The variations in velocity may be significant if the timing of contaminant break-through is critical, however this condition is not of interest for evaluating an OWTS. Contaminant break-through is generally not critical for an OWTS because the long term transport behavior of the system is more important than the behavior at start-up when considering potential contamination of receptors. With respect to transverse advection the cell-by-cell flow file created by MODFLOW revealed that it did not occur for this case. One possible explanation is that the random nature of the hydraulic conductivity field does not create a situation where multiple cells with similar hydraulic conductivities are adjacent and thus advection remains one-dimensional.

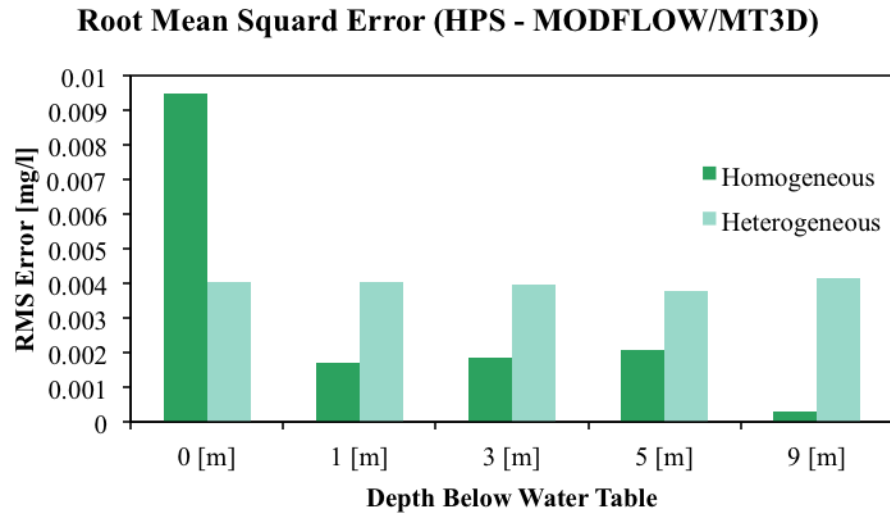


**Figure 2.3**  
**Comparison of the root mean squared error between the HPS predicted concentrations and the numerical models with a homogeneous and heterogeneous hydraulic conductivity fields. It is unknown why a larger discrepancy exists between predictions from the numerical model with a homogeneous hydraulic conductivity field and the HPS solution at the aquifer surface**



## Section 3.0

### Revisions and Improvements to the Aquifer Model

---

Several revisions were incorporated to into the HPS saturated zone module to improve ease of implementation and improve plume predictions.

#### 3.1 Revisions to Saturated Denitrification Rates

First order reaction kinetics are utilized to simulate the denitrification process which is the generally accepted method (McCray et al., 2005). The reported first order rates by McCray et al. (2005) ranged from 0.004 to 2.27 d<sup>-1</sup>. However during model performance evaluation and calibration it was observed that not only is the denitrification rate a very sensitive parameter, much lower rates were required to capture observed plume extents.

Additional evaluation of literature values revealed that the range of first order denitrification rates in McCray et al. (2005) included literature reported values from a wide range of saturated conditions such as fissured limestone, clay, and gravel (Kirkland, 2001). Another difficulty is that denitrification rates are known to follow both zero-order and first-order kinetics. As Tucholke (2007) found, most rates reported in the literature are zero order and associated with agricultural studies (e.g., rates expressed in terms of mass nitrogen per area per time). Conversion of zero-order rates to first-order rates requires making some assumptions (e.g., representative soil depth, consideration of factors affecting denitrification [temperature, pH, available organic carbon, soil texture, etc.]) and adds uncertainty to the assumed denitrification rate.

Figure 3.1 is a cumulative frequency diagram of first order denitrification rates for saturated (100% water filled porosity) sands in Florida adapted from Bradley et al. 1992 (temperature corrected to 25°C, Tucholke 2007). As shown on the CFD, when considering only first order denitrification rates specific to Florida aquifers, the range of rates includes rates lower than 0.004 d<sup>-1</sup>. Thus, the default denitrification rate populated into the saturated zone module was the 25th percentile value of 0.002 d<sup>-1</sup>. While this rate is conservative (limits denitrification), it was supported by model corroboration. A higher or lower denitrification rate may be appropriate based on site conditions.

c:\4237-001R006\Wpdocs\Report\Final

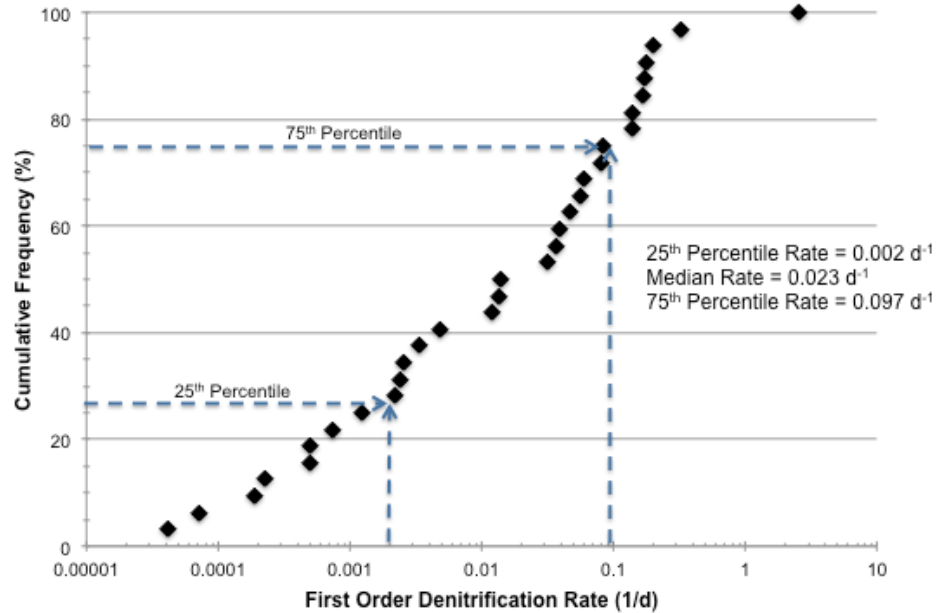


Figure 3.1

**Saturated Denitrification Rates Adapted from Bradley et al., 1992 (Tucholke 2007).**

### 3.2 Capability to Run the Combined Aquifer-Complex Soil Model Together

A new STUMOD-HPS module was added designed to run unsaturated and saturated zone modules all in one run and to generate both saturated and unsaturated zone outputs. Users can generate outputs at the water table and at a down gradient distance from the soil treatment unit in one run. As with the individual module runs, the STUMOD-FL module calculates boundary concentration for the HPS module. HPS module calculates mass loading and concentration at a distance the user specifies. The combined module can also interact with the user during the run by asking the user if they want to use the outputs from STUMOD-FL or if they want to use different inputs.

A new page is added to show the outputs from combined STUMOD-HPS run. The outputs from the unsaturated and saturated zone modules are shown in Figure 3.2 with 'Model Outputs' at the top of the page and 'Model Graphical Outputs' at the bottom of the page. The mass loadings and percent mass remaining are provided at the infiltrative surface, water table, and user specified down gradient location.



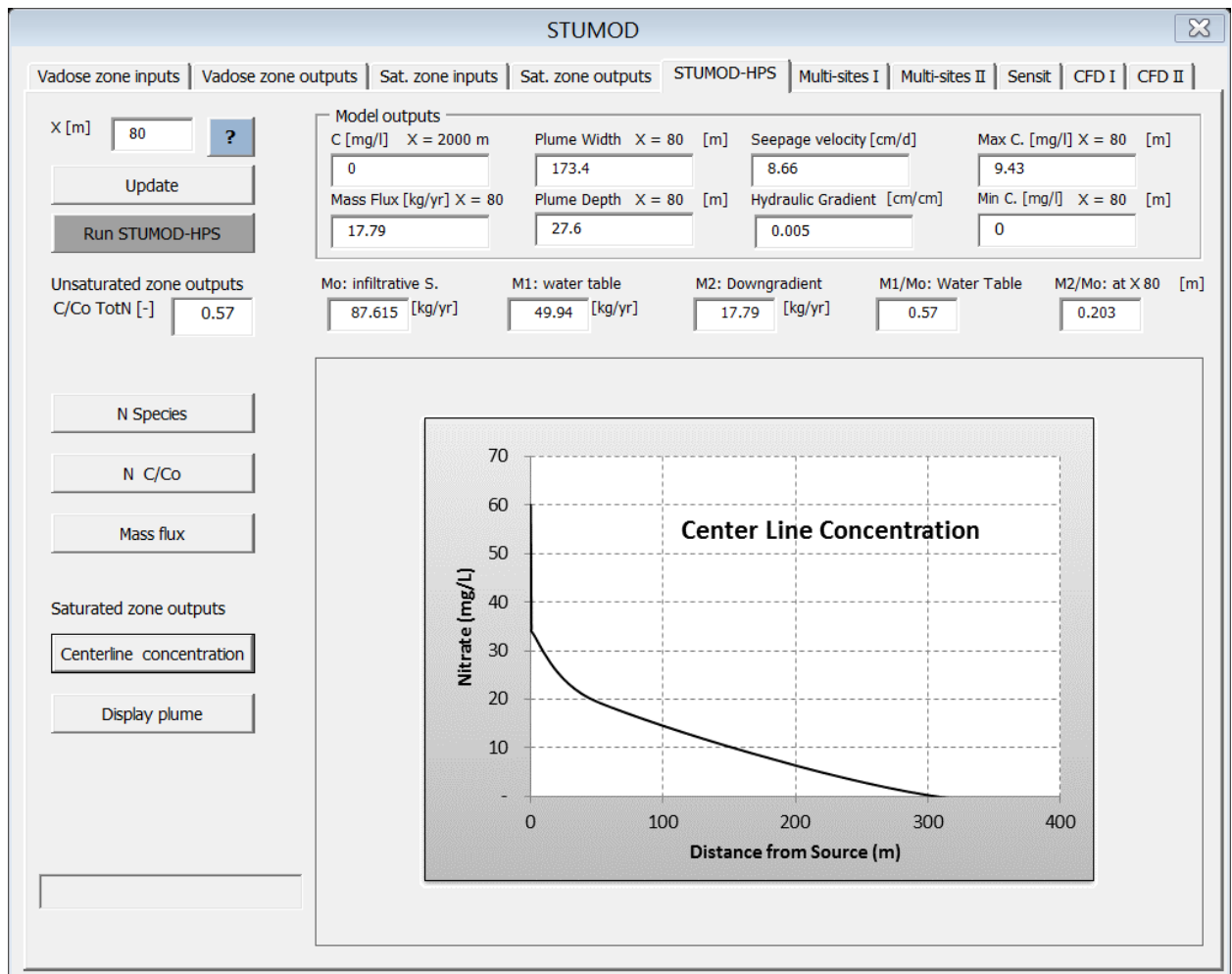


**Figure 3.2**  
**STUMOD-HPS combined module GUI.**

The combined module graphical user interface (GUI) allows the user to load values used in the previous run, use default values, or input new values by going to the input box for each parameter. Values used in the previous run are stored in an Input Summary Worksheet and can be accessed by the user.

### 3.3 Improvements to the Graphical User Interface (GUI)

Numerous errors within the GUI have been corrected based on comments received on the draft model. These revisions include:

- correction of spelling errors,
- correction of mislabeled input fields and pop-up notes,
- making the axis consistent on all graphs,
- removal of horizontal plume visualization, and
- elimination of conflict between the gradient and flow direction with "Run Ground-water Model" button.

In addition, additional capability has been added to improve the ease of use. These additional capabilities include:

- simplifying use by grouping the input parameters into categories (Figure 3.3),
- adding a help button "?" to each input parameter category so users can get a description of each category of inputs,
- adding a "back to GUI" action button on data worksheets,
- adding a "Default Value" button,
- allowing users to select default parameters or update any individual parameter by choosing the input category submenu and changing a value,
- defining columns and cells on various worksheets, and
- adding a new worksheet that allows export of the data more easily.

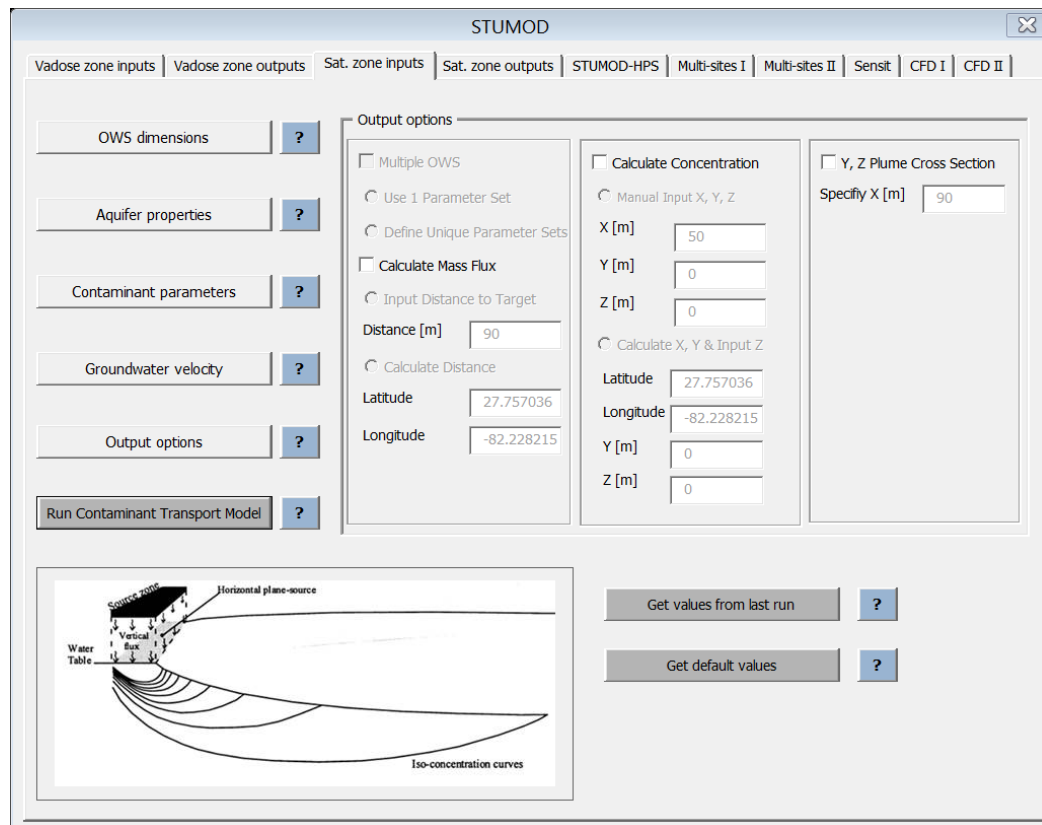


**Figure 3.3**  
STUMOD-FL-HPS GUI showing grouping of input parameters.



## Section 4.0

### Corroboration of Combined Aquifer-Complex Soil Model to Field Data

---

Corroboration of the individual vadose zone and aquifer modules have been described previously in the FOSNRS Task D.9 and Task D.12 reports. The corroboration discussed here used the combined model (STUMOD-FL-HPS) specifically to compare data collected during Task C at home sites and the GCREC S&GW test facility.

Users will likely evaluate model performance by comparing STUMOD-FL-HPS outputs to available field data. However, it is vital to understand the requirements for the quality and quantity of field data needed in order to make a valid comparison. Development of STUMOD-FL-HPS required simplifying assumptions based on a conceptual model that does not capture the variability often observed in field conditions. For example, water use and effluent concentrations are known to vary widely depending on household activities. While the septic tank attenuates these variations, it is not uncommon for water use to range between 120 and 250 L/capita/d and total nitrogen concentrations to vary between 40 and 90 mg-N/L (Lowe et al., 2009). Indeed, at homesite CHS2, daily water use ranged between 97 and 360 gallons/day (excluding days when the outdoor pool was filled) and at the GCREC S&GW effluent ammonium nitrogen concentrations ranged between 50 and 80 mg-N/L. The impact of these variations on HLR and subsurface nitrogen measurements cannot be captured by a model such as STUMOD-FL-HPS which assumes steady state behavior. Heterogeneities in natural systems and climate variations pose similar challenges.

This limitation is generally mitigated by averaging the observed data to approximate steady-state behavior. Increasing the frequency (both temporal and spatial) and duration of observations improves the steady-state approximation, but comes at a cost that is rarely supported. As an example, the nitrogen input to groundwater is directly a result of nitrogen transformation in the unsaturated soil. However, vadose zone monitoring requires a high degree of technical understanding in the field while also being time consuming and expensive. Such monitoring greatly improves the ability to corroborate a model to a field site, but is not recommended for general practitioners or homeowners. Vadose zone monitoring was intentionally conducted at the GCREC S&GW, but not



home sites in part due to budget constraints but also to help show how uncertainty is added to model performance assessment when observed data is limited.

Even in very controlled sites, such as the GCREC S&GW facility where observations are relatively plentiful, the conceptual model that is the basis of STUMOD-FL-HPS requires simplifications. An example is ammonium sorption controlled by cation exchange processes that are not incorporated into the model but believed to be at least partially responsible for variations in nitrogen field observations (Parzen, 2007; Siegrist et al., 2014). In addition, research has shown that while ammonium sorption typically follows a linear isotherm in field soils where the concentrations of ammonium are relatively low ( $<22 \text{ mg-N L}^{-1}$ ) (DeSimone and Howes, 1998), a nonlinear adsorption relationship is typically assumed under high concentration conditions (van Raaphorst and Malschaert, 1996; Laima et al., 1999; Fernando et al., 2005). This phenomenon may impact the magnitude of sorption in the STU and subsequent transformation processes. The complexity of ammonium sorption in soils is not accounted for in STUMOD-FL but would require a geochemical model to incorporate more detailed processes (e.g., ammonium cation exchange).

#### **4.1 Corroboration of STUMOD-FL-HPS to Home Site Data**

Observed field data at the CHS2 home site were compared to STUMOD-FL-HPS outputs. For corroboration, model predictions were compared to field observations both before and after installation of the PNRS at the home. To approximate steady state conditions, the observed data from all sampling events were averaged (before PNRS = SE1, SE2, SE3, SE4, and SE5; After PNRS = SE6, SE7, SE8, SE9, SE10, SE11, and SE12). The effects of rainfall, plant uptake, and ET were not considered. Model input parameters for simulations before installation of PNRS are provided in Table 4.1. Model input parameters for simulations after installation of PNRS are provided in Table 4.2.

**Table 4.1**  
**Parameter Values used for STUMOD-FL-HPS Corroboration to CHS2 Home Site**  
**(before installation of PNRs)\***

Parameter	Symbol (units)	Input Value
Number of trenches	-	7
Trench width	B (ft)	2.83
Trench length	L (ft)	37.82
Total infiltrative surface area	- (ft <sup>2</sup> )	750
Unsaturated denitrification rate	K <sub>dnt max</sub> (mg-N L <sup>-1</sup> d <sup>-1</sup> )	3.32
Depth to groundwater	D (cm)	54.5
Hydraulic loading rate	HLR (cm/d)	0.68
Effluent ammonium concentration	C <sub>o</sub> NH <sub>4</sub> (mg-N/L)	60.0
Effluent nitrate concentration	C <sub>o</sub> NO <sub>3</sub> (mg-N/L)	0.06
Saturated hydraulic conductivity	K <sub>sat</sub> (cm/d)	92.96
Porosity	n (-)	0.38
Gradient	grad (m/m)	0.008
Saturated denitrification rate	Decay Rate (d <sup>-1</sup> )	0.002
Carbon input	- (as mg BOD <sub>5</sub> /L)	115.0

\* Default parameters for "less permeable sand" were used based on the K<sub>sat</sub> determined at the site from slug tests. Soils were characterized as Myakka and EauGallie fine sands. Depth to the infiltrative surface was estimated at 64cm.

**Table 4.2**  
**Parameter Values used for STUMOD-FL-HPS Corroboration to CHS2 Home Site**  
**(after installation of PNRs)\***

Parameter	Symbol (units)	Input Value
Number of beds (L- shaped effluent drip irrigation area)	-	2
Bed 1 dimensions	- (ft <sup>2</sup> )	112
Bed 2 dimensions	- (ft <sup>2</sup> )	503
Total infiltrative surface area	- (ft <sup>2</sup> )	615
Unsaturated denitrification rate	K <sub>dnt max</sub> (mg-N L <sup>-1</sup> d <sup>-1</sup> )	3.32
Depth to groundwater	D (cm)	64.0
Hydraulic loading rate	HLR (cm/d)	0.83
Effluent ammonium concentration	C <sub>o</sub> NH <sub>4</sub> (mg-N/L)	0.33
Effluent nitrate concentration	C <sub>o</sub> NO <sub>3</sub> (mg-N/L)	0.61
Saturated hydraulic conductivity	K <sub>sat</sub> (cm/d)	92.96
Porosity	n (-)	0.38
Gradient	grad (m/m)	0.011
Saturated denitrification rate	Decay Rate (d <sup>-1</sup> )	0.002
Carbon input	- (as mg BOD <sub>5</sub> /L)	18.0

\* Default parameters for "less permeable sand" were used based on the K<sub>sat</sub> determined at the site from slug tests. Soils were characterized as Myakka and EauGallie fine sands. Depth to the infiltrative surface was estimated at 25 cm.

O:\44237-001R005\Wpdocs\Report\Final

Nitrate concentrations varied with sampling depth (Table 4.3). However, based on averaged nitrate concentrations observed at the site, generally the concentrations at shallow depth (5 to 6 ft) were greater than concentrations at the intermediate sampling depth (7 to 8 ft) and very little nitrogen was detected at the deeper locations (10 to 12 ft). As with nitrogen concentrations, the water table varied, but was generally relatively shallow - between 2 and 5.5 ft bgs. Due to the water table fluctuations and because the most shallow piezometers were installed at 5ft bgs, the nitrate concentrations from the shallow sampling depth were assumed to represent the top of the groundwater and were compared to STUMOD-FL-HPS values predicted at  $z = 0$ . The nitrate concentrations at the intermediate sampling depth were compared to STUMOD-FL-HPS values predicted at  $z = 2$  ft (i.e., 2 ft below the water table) and the nitrate concentrations at the deeper sampling depth were compared to STUMOD-FL-HPS values predicted at  $z = 4$  ft (4 ft below the water table).

**Table 4.3**  
**STUMOD-FL-HPS Corroboration Results at CHS2 before PNRS Installation.**

Loc ID	Depth (ft)	Distance <sup>1</sup> (m)	HLR (cm/d)	Gradient	Denit Rate (d <sup>-1</sup> )	Field Obs NO <sub>3</sub> (mg-N/L)	Model NO <sub>3</sub> Conc (mg-N/L)
Shallow Completions							
A07	6	13.0	0.68	0.008	0.002	6.05	3.43
A07	6	13.0	1.58	0.008	0.002	6.05	26.27
B08	5	25.5	0.68	0.008	0.002	21.8	2.96
B08	5	25.5	1.58	0.008	0.002	21.8	22.63
C06	5	43.1	0.68	0.008	0.002	12.14	0.61
C06	5	43.1	1.58	0.008	0.002	12.14	4.69
D07	6	44.0	0.68	0.008	0.002	8.52	0.57
D07	6	44.0	1.58	0.008	0.002	8.52	4.36
C08	5	46.0	0.68	0.008	0.002	6.38	0.48
C08	5	46.0	1.58	0.008	0.002	6.38	3.70
D04	5	48.0	0.68	0.008	0.002	11.87	0.41
D04	5	48.0	1.58	0.008	0.002	11.87	3.14
Intermediate Completions							
A07	8	13.0	0.68	0.008	0.002	20	1.15
A07	8	13.0	1.58	0.008	0.002	20	26.00
B08	7	25.5	0.68	0.008	0.002	9.48	1.05
B08	7	25.5	1.58	0.008	0.002	9.48	8.04
C06	7	43.1	0.68	0.008	0.002	1.51	0.34
C06	7	43.1	1.58	0.008	0.002	1.51	2.58
D07	8	44.0	0.68	0.008	0.002	0.77	0.32
D07	8	44.0	1.58	0.008	0.002	0.77	2.43
C08	7	46.0	0.68	0.008	0.002	17.87	0.28
C08	7	46.0	1.58	0.008	0.002	17.87	2.11
D04	7	48.0	0.68	0.008	0.002	3.97	0.24
D04	7	48.0	1.58	0.008	0.002	3.97	1.84
Deep Completion							
PZ06	12	8.4	0.68	0.008	0.002	13.42	0.10
PZ06	12	8.4	1.58	0.008	0.002	13.43	0.14
A07	11	13.0	0.68	0.008	0.002	0.37	0.10
A07	11	13.0	1.58	0.008	0.002	0.37	0.14
B08	10	25.5	0.68	0.008	0.002	0.08	0.10
B08	10	25.5	1.58	0.008	0.002	0.08	0.14
C06	10	43.1	0.68	0.008	0.002	0.07	0.05
C06	10	43.1	1.58	0.008	0.002	0.07	0.08
D07	11	44.0	0.68	0.008	0.002	0.14	0.05
D07	11	44.0	1.58	0.008	0.002	0.14	0.07
C08	10	46.0	0.68	0.008	0.002	0.07	0.05
C08	10	46.0	1.58	0.008	0.002	0.07	0.07
D04	10	48.0	0.68	0.008	0.002	0.10	0.04
D04	10	48.0	1.58	0.008	0.002	0.10	0.06

<sup>1</sup> x,y distance from the center of the infiltrative surface



During corroboration different parameters were adjusted resulting in improved model predictions of the down gradient plume. The parameters evaluated/altered during the corroboration were hydraulic loading rate and saturated zone denitrification rate. Other parameter values were not altered. When a median denitrification rate of 0.023/d (see Figure 3.1) was used the model predicted nitrate concentrations were much lower than observed concentrations. Adjusting the saturated denitrification rate to the 25 percentile value of 0.002/d improved the corroboration, but did not capture all of the differences between the model predictions and the field observation. It was known that the water use at the home site varied during Task C monitoring. Based on this site understanding, two HLRs were evaluated: 0.68 to 1.58 cm/d (well within the observed variations in HLR due to water use fluctuations). For model corroboration using the average HLR of 0.68 cm/d, nitrate concentrations were under predicted by STUMOD-FL-HPS at all sampling depths (Figure 4.1). By adjusting only the HLR from 0.68 to 1.58 cm/d, model performance was improved as shown in Figure 4.2.

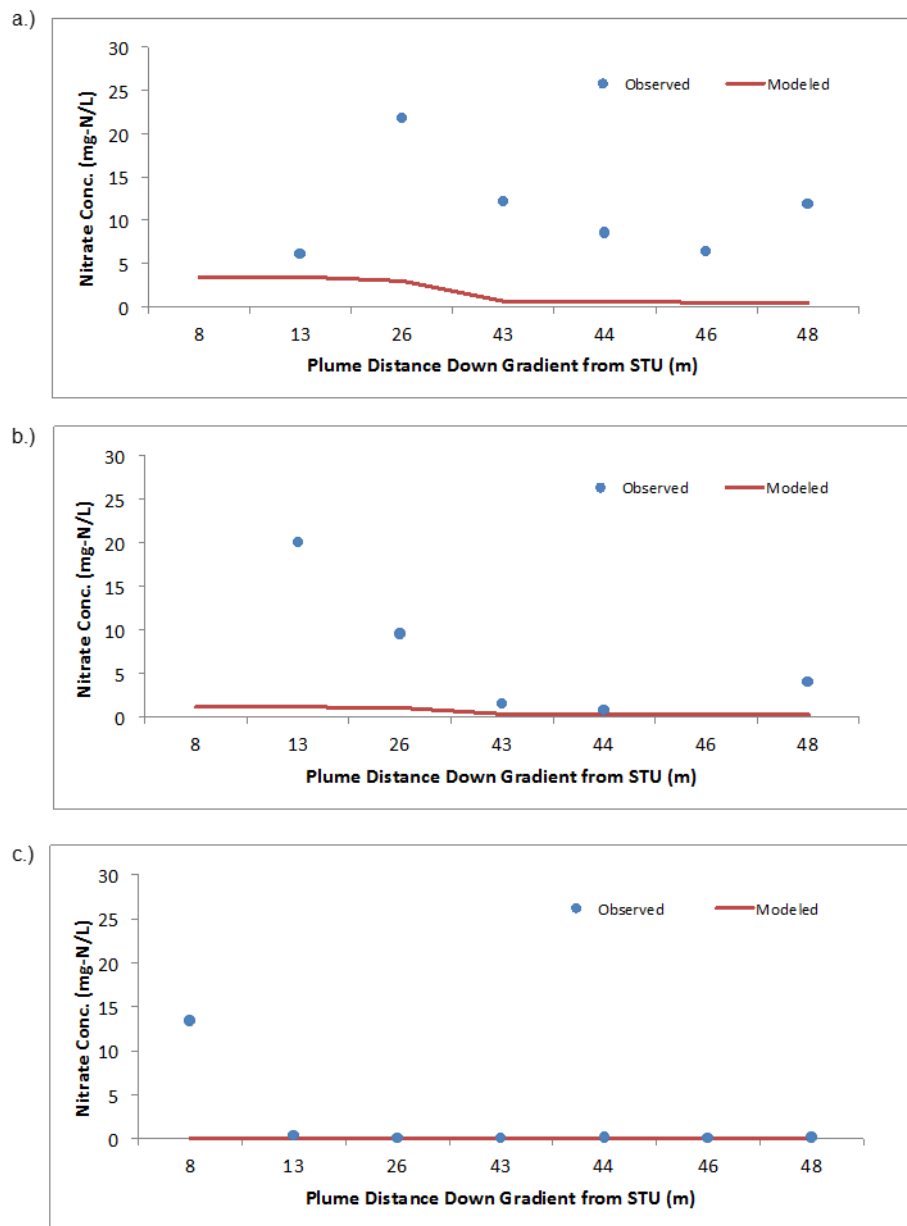


**Figure 4.1**  
**Comparison of STUMOD-FL-HPS predictions to field observations using averaged model inputs (Table 4.1). a = shallow depths, b = intermediate depths, and c = deep depths.**

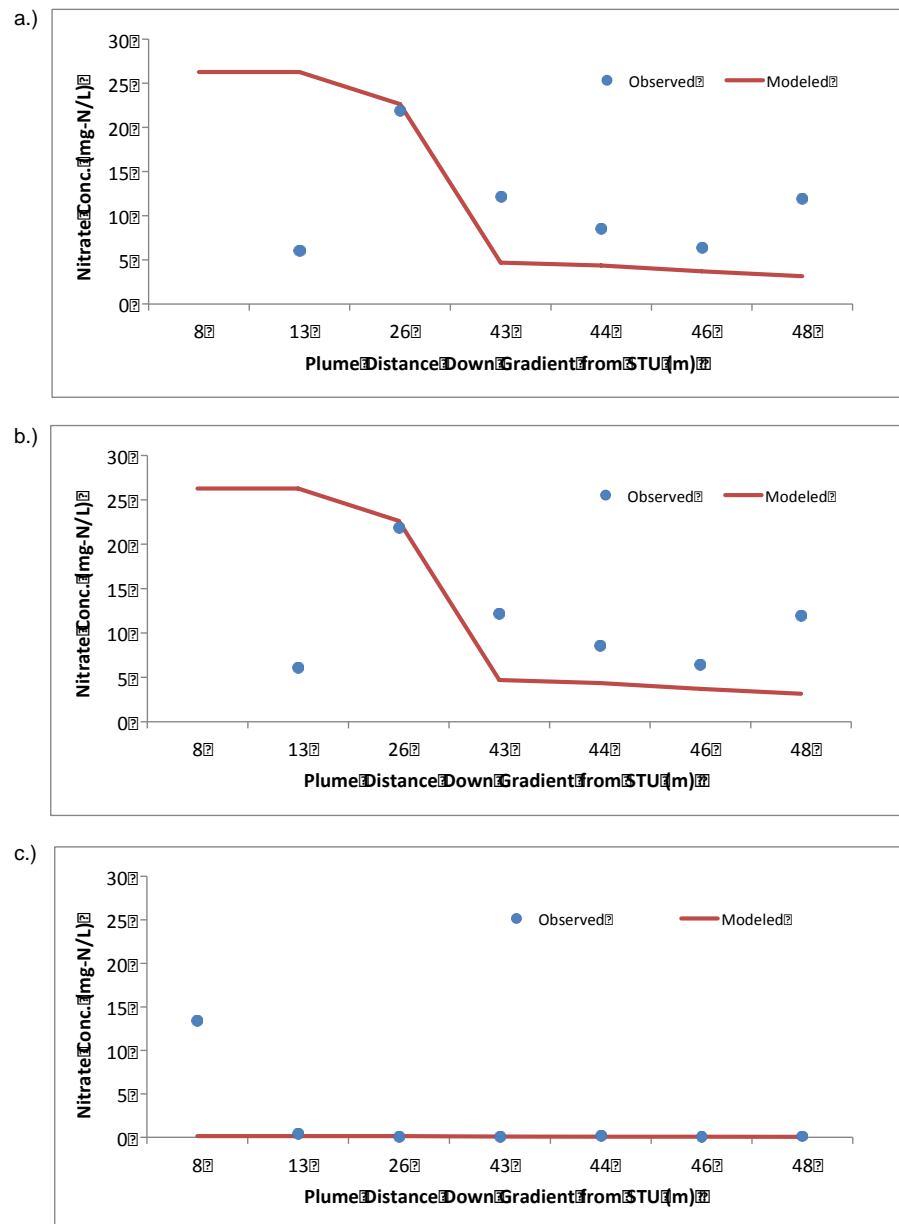


**Figure 4.2**  
**Comparison of STUMOD-FL-HPS predictions to field observations adjusting the HLR input (from 0.68 to 1.58 cm/d). a = shallow depths, b = intermediate depths, and c = deep depths.**

O:\44237-001R005\Wpdocs\Report\Final

Although, parameter adjustments could not capture the variability observed in the field, this is not surprising based the limitations of the conceptual model. Figure 4.3 is taken from the FOSNRS CHS2 Task C.26 Summary and Close-out report and shows the plume variability as well as how sample locations control the Surfer graphical software generation of the plume extent. Non-uniform changes in both depth and distance are shown requiring a more complex numerical model that captures these heterogeneities to better represent the field data using a single set of parameter adjustments.

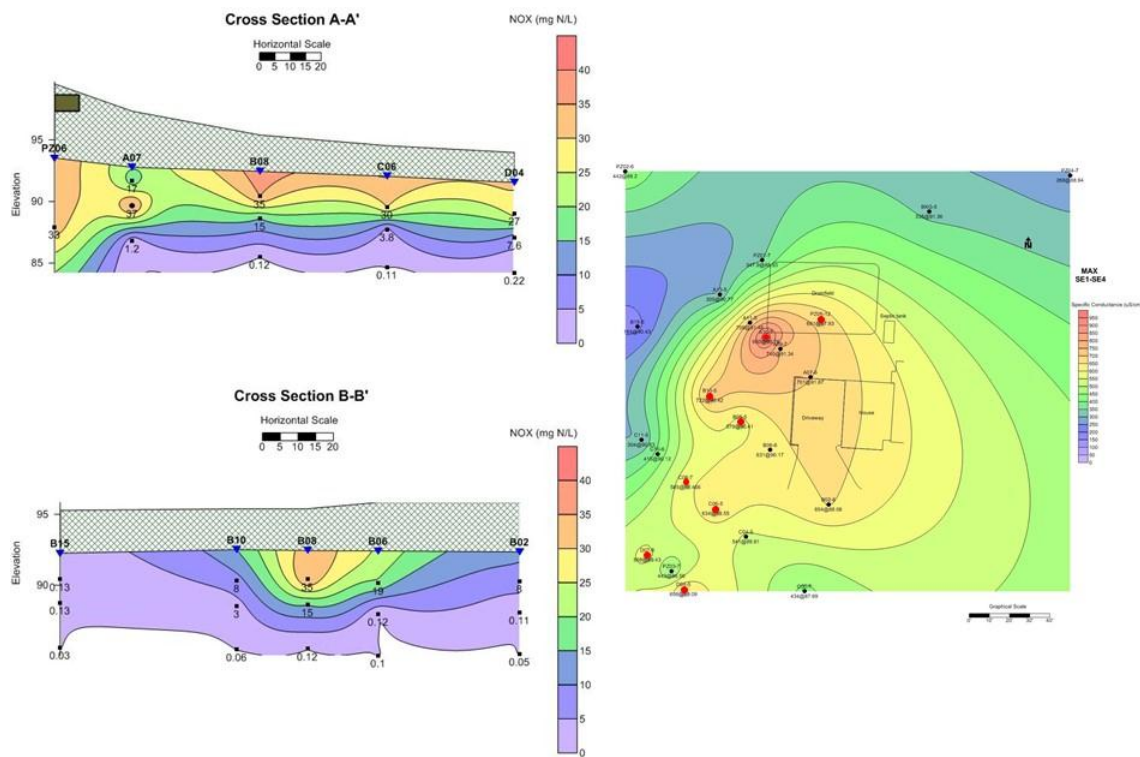


**Figure 4.3**  
**Surfer generated plume illustrations using maximum NO<sub>x</sub> concentrations (cross sections) and maximum specific conductance (plan view).**

The inputs shown in Table 4.2 were used to evaluate STUMOD-FL-HPS performance after installation of PNRS. While the average total nitrogen input to infiltrative surface after PNRS installation was 0.94 mg-N/L (Table 4.2) most of the nitrate concentration



observations in the groundwater were higher (Table 4.4). This is attributed to the step change in operation (i.e., before PNRS installation to after PNRS installation), but a longer response time in the saturated zone than was captured by the field sampling. Thus, as expected when a total nitrogen input concentration of 0.94 mg-N/L was used, the model could not match observed concentrations considerably greater than the input concentration. However, the model could match several observations down gradient as shown in Figure 4.4. The accuracy of STUMOD-FL-HPS predictions is increased after a distance of 2 times the length of the infiltrative surface and as a consequence, the closest two data points could not be predicted. To compensate for the problems with the input concentration, a modified scenario is illustrated (Figure 4.4, dashed line) where the input concentration and the locations within the infiltrative surface area were set equal to the mean observed concentration 3.8 mg-N/L.

**Table 4.4**  
**STUMOD-FL-HPS Corroboration Results at CHS2 after PNRS Installation.**

Loc ID	Depth (ft)	Distance <sup>1</sup> (m)	HLR (cm/d)	Gradient	Denit Rate (d. <sub>1</sub> )	Field Obs NO <sub>3</sub> (mg-N/L)	Model NO <sub>3</sub> Conc (mg-N/L) <sup>2</sup>
PZ07	7	8.2	0.83	0.011	0.002	3.78	-
PZ08	7	3.3	0.83	0.011	0.002	3.67	-
PZ09	7	27.0	0.83	0.011	0.002	7.79	0.019
A07	6	20.5	0.83	0.011	0.002	0.41	
A07	8	20.5	0.83	0.011	0.002	2.72	
A07	11	20.5	0.83	0.011	0.002	0.03	
averaged						1.73	0.019
B08	5	32.8	0.83	0.011	0.002	0.30	
B08	7	32.8	0.83	0.011	0.002	0.39	
B08	10	32.8	0.83	0.011	0.002	0.03	
averaged						0.50	0.016
C06	5	47.5	0.83	0.011	0.002	0.02	
C06	7	47.5	0.83	0.011	0.002	0.02	
C06	10	47.5	0.83	0.011	0.002	0.03	
averaged						0.45	0.009
D04	5	54.5	0.83	0.011	0.002	0.55	
D04	7	54.5	0.83	0.011	0.002	0.02	
D04	10	54.5	0.83	0.011	0.002	0.03	
averaged						0.49	0.006

<sup>1</sup> x,y distance from the center of the infiltrative surface

<sup>2</sup> Because nitrate concentrations were so low, the average value predicted by the model at the specific distance was compared to the averaged observed data value.

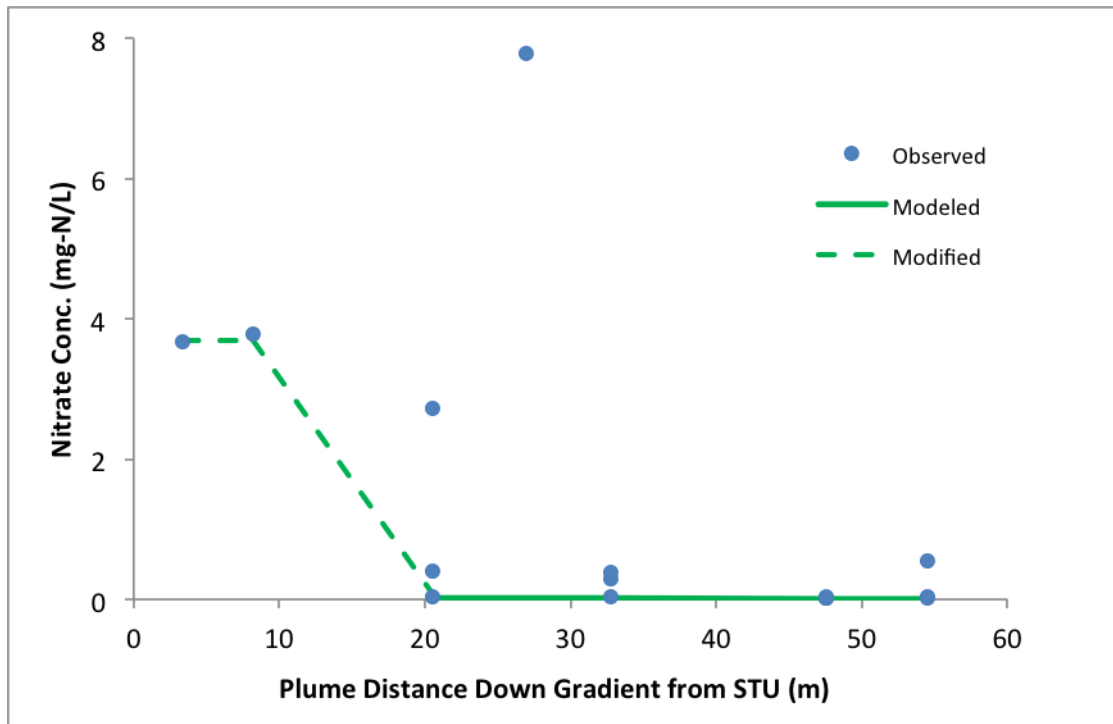


**Figure 4.4**  
**Comparison of STUMOD-FL-HPS predictions to field observations after PNRS installation.**

#### 4.2 Corroboration of STUMOD-FL-HPS to S&GW Data

As part of FOSNRS Task D.9, observed field data representing field conditions were compared to STUMOD-FL outputs. There are 6 test areas (mini-mounds) at the GCREC S&GW test facility receiving either septic tank effluent (STE) or nitrified effluent delivered to the soil via a pressure dosed mound or a shallow drip dispersal system. Corroboration of the vadose zone module was conducted for Test Areas 1, 2, 3 and 4 as well as to the USF Lysimeter Station. Results from corroboration indicate that STUMOD-FL agrees with the conceptual model and that model outputs generally agree with field observations. Specifically, ammonium is removed quickly within the soil profile and subsequently nitrified with generally decreasing nitrate concentrations with depth. However, nitrate predictions were found to be more conservative compared to field data (i.e., STUMOD-FL predicted nitrate concentrations relatively higher than field observations). This same trend was demonstrated using HYDRUS-2D. This observation of higher predicted nitrate concentrations was particularly pronounced at shallow depth and is attributed to opera-

O:\4237-001R005\Wpdocs\Report\Final

tional variability and environmental factors (including rainfall) that would have a more pronounced effect at a shallow depth.

As part of FOSNRS Task D.12, observed field data representing field conditions at the GCREC mound were compared to HPS outputs. Results from corroboration resulted in an increased calibrated dispersivity value and a lower denitrification rate. This was attributed to denitrification occurring to a greater extent than the calibrated denitrification coefficient suggests but may be limited, a depressed calibrated denitrification rate due to the agricultural nitrate plume, and complex advection fields within the aquifer (the HPS solution only considers one dimensional advection though two or three dimensional advection is likely occurring).

As part of FOSNRS Task D.13, observed field data at the GCREC S&GW facility were compared to STUMOD-FL-HPS outputs. For corroboration, model predictions were compared to field observations during the last sampling event (SE6) conducted in July 2013. Corroboration to earlier sampling events was not attempted since the system became operational in July 2012 and earlier sampling events are not assumed to represent steady state. The effects of rainfall, plant uptake, and ET were not considered. Model input parameters are provided in Table 4.5.

**Table 4.5**  
**Parameter Values used for STUMOD-FL-HPS Corroboration to TA1\***

Parameter	Symbol (units)	Input Value
Trench width	B (cm)	121.92
Trench length	L (cm)	365.76
Unsaturated denitrification rate	$K_{dnt\ max}$ (mg-N L <sup>-1</sup> d <sup>-1</sup> )	3.32
Depth to groundwater	D (cm)	75.6
Hydraulic loading rate	HLR (cm/d)	3.26
Effluent ammonium concentration	$C_o\ NH_4$ (mg-N/L)	57.5
Effluent nitrate concentration	$C_o\ NO_3$ (mg-N/L)	0.01
Saturated hydraulic conductivity	$K_{sat}$ (cm/d)	352.6
Porosity	n (-)	0.38
Gradient	grad (m/m)	0.006
Saturated denitrification rate	Decay Rate (d <sup>-1</sup> )	0.002

\* Default parameters for a "less permeable sand" were used. The soils at the S&GW facility have been classified as Seffner sand. Depth to the infiltrative surface was estimated at 45 cm.

The observed data showed nitrate concentrations considerably lower at the 9 ft depth compared to 11 ft or 16 ft depths. Using model default values and the inputs shown in Table 4.5, the model predicted values could be matched to the lower nitrate concentra-

tions observed at 9 ft sampling point (Table 4.6 and Figures 4.5 and 4.6). Model predicted values were considerably lower compared to the observations at 11 and 16 ft sampling points. However, the model predictions at 11 and 16 ft depths could be improved by using relatively lower dispersivity values as shown in Table 4.7 and Figures 4.7 and 4.8).

**Table 4.6**  
**STUMOD-FL-HPS Simulation Output Summary using High Dispersivity Values.\***

Location ID	Observation Depth (ft)	Distance from IS (m)	Observed NO <sub>3</sub> Conc. (mg-N/L)**	Predicted NO <sub>3</sub> Conc. (mg-N/L)
TA1-PZ-09-I7	9	11.3	2.10	3.95
TA1-PZ-09-N3	9	16.6	4.20	3.60
TA1-PZ-09-M9	9	18.0	1.10	3.45
TA1-PZ-09-O7	9	40.4	1.80	3.16
TA1-PZ-09-RS16	9	41.4	3.30	1.00
TA1-PZ-09-RS18	9	45.2	0.36	0.82
TA1-PZ-11-J4	11	9.12	34.0	3.97
TA1-PZ-11-L2	11	12.2	49.0	3.92
TA1-PZ-11-L3	11	12.3	36.0	3.92
TA1-PZ-11-L4	11	12.6	31.0	3.91
TA1-PZ-11-L5	11	13.3	17.0	3.87
TA1-PZ-11-EF2	16	11.5	22.0	3.95
TA1-PZ-16-I7	16	16.6	19.0	3.60
TA1-PZ-16-N3	16	18.0	22.0	3.46
TA1-PZ-16-M9	16	20.2	16.0	3.19
TA1-PZ-16-O7	16	41.4	3.20	1.00
TA1-PZ-16-RS16	16	45.3	11.0	0.82

\* x-dispersivity ( $D_x$ ) = 1000; y-dispersivity ( $D_y$ ) = 100; and z-dispersivity ( $D_z$ ) = 10

\*\* observed values during SE6, July 2013

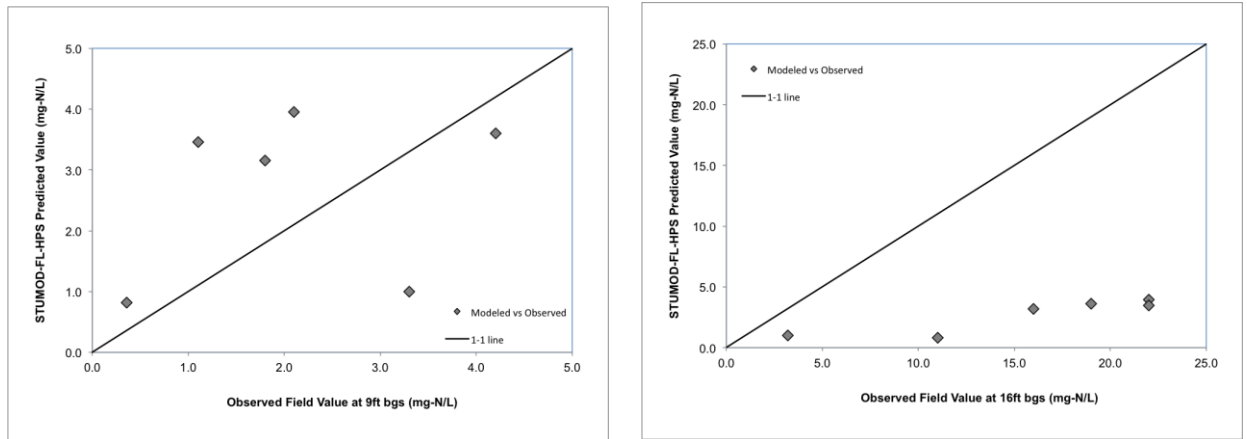


Figure 4.5

Model fit to observed data at the 9 and 16ft depths using high dispersivity values.

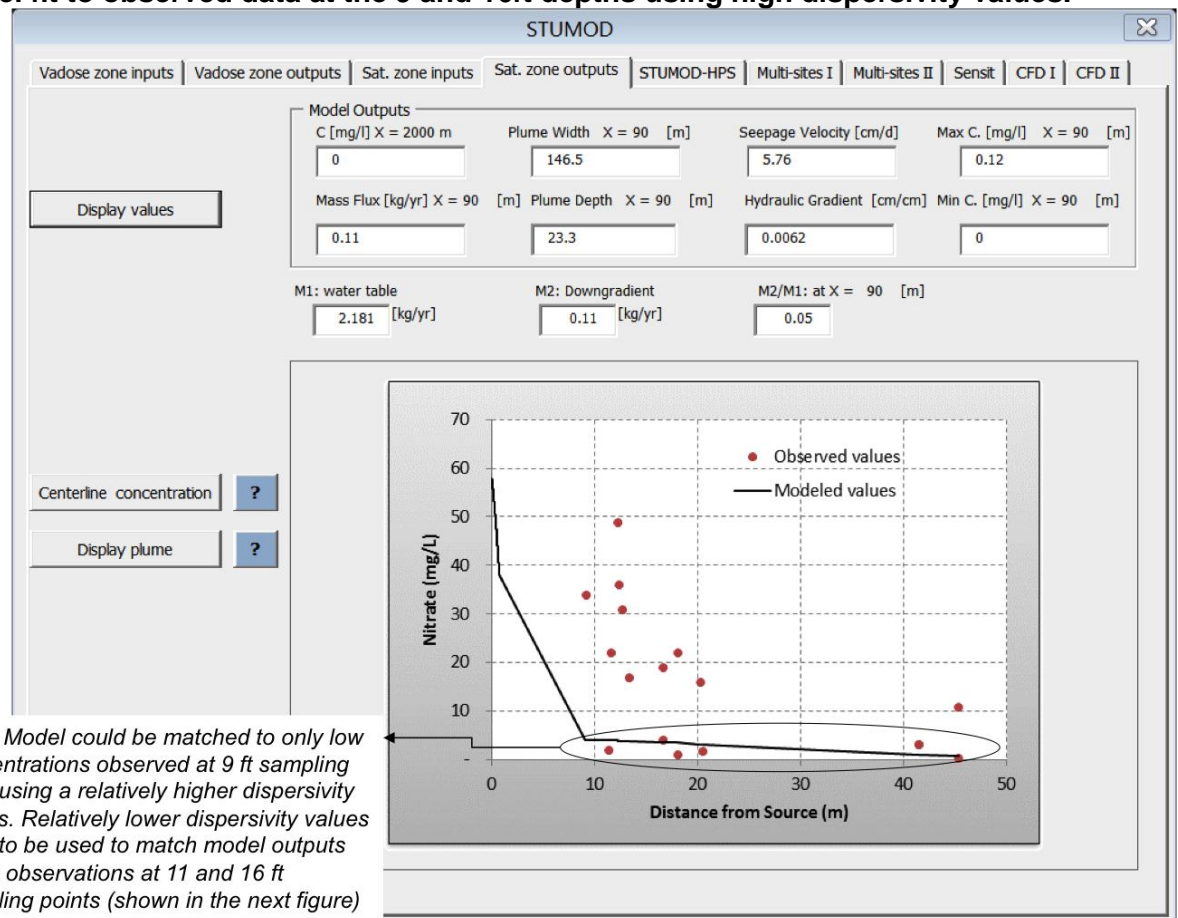


Figure 4.6

Model output using high dispersivity values.

**Table 4.7**  
**STUMOD-FL-HPS Simulation Output Summary using Low Dispersivity Values.\***

Observation Depth (ft)	Distance from IS (m)	Observed NO <sub>3</sub> Conc. (mg-N/L)	Predicted NO <sub>3</sub> Conc. (mg-N/L)
9	11.3	2.10	31.96
9	16.6	4.20	17.86
9	18.0	1.10	15.74
9	40.4	1.80	12.84
9	41.4	3.30	3.24
9	45.2	0.36	2.63
11	9.12	34.0	31.91
11	12.2	49.0	28.34
11	12.3	36.0	28.25
11	12.6	31.0	27.80
11	13.3	17.0	26.68
16	11.5	22.0	29.37
16	16.6	19.0	21.14
16	18.0	22.0	18.99
16	20.2	16.0	15.83
16	41.4	3.20	3.95
16	45.3	11.0	3.21

\* x-dispersivity ( $D_x$ ) = 500; y-dispersivity ( $D_y$ ) = 50; and z-dispersivity ( $D_z$ ) = 1

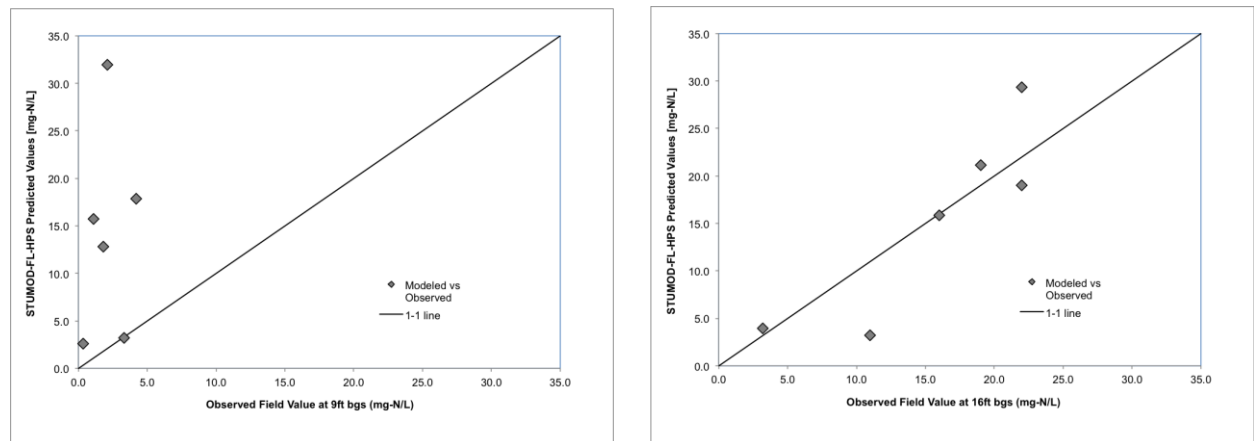


**Figure 4.7**  
**Model fit to observed data at the 9 and 16ft depths using high dispersivity values.**

O:\44237-001R005\Wpdocs\Report\Final



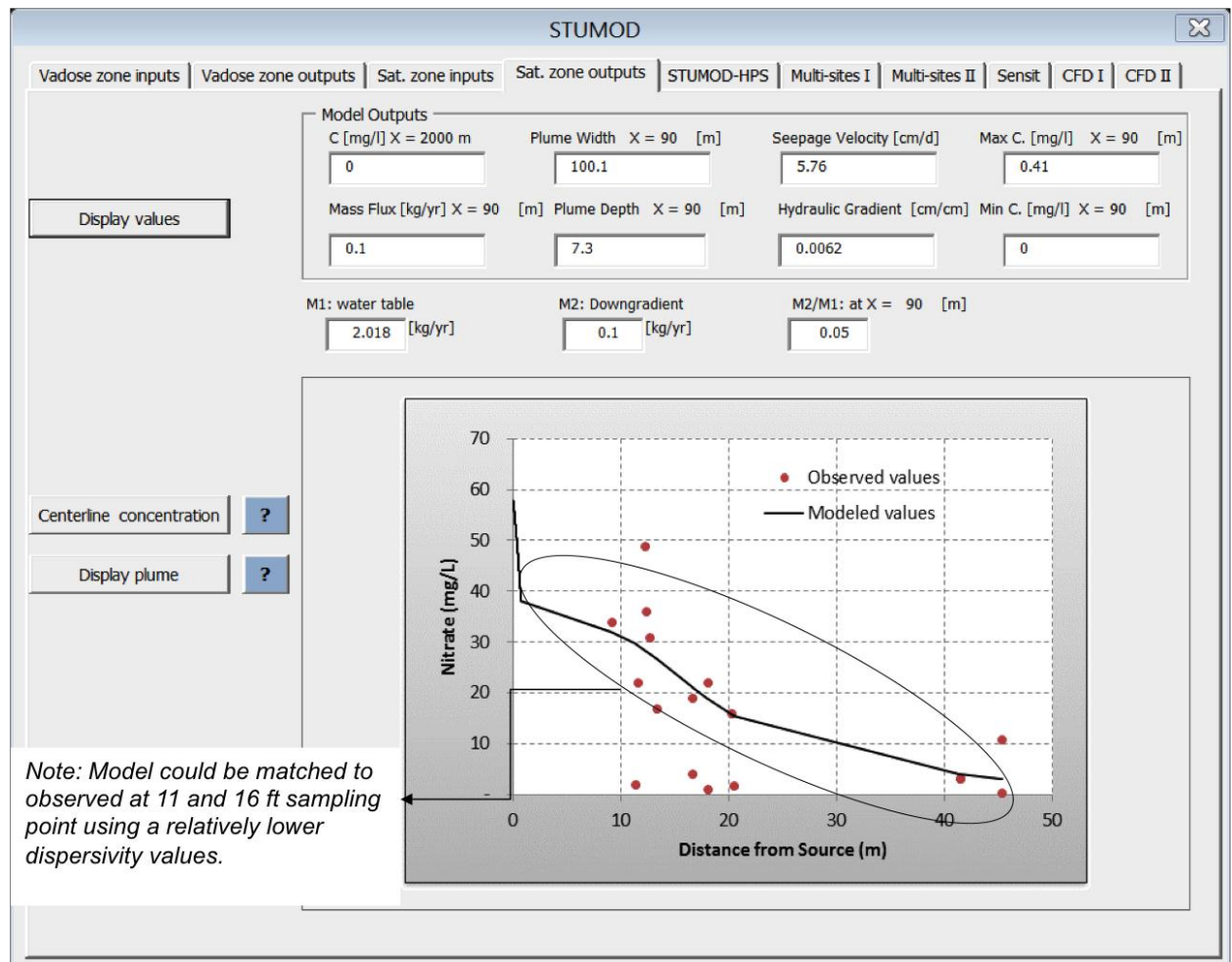


**Figure 4.8**  
**Model output using low dispersivity values.**

### 4.3 Corroboration of STUMOD-FL-HPS Summary

During corroboration different parameters could be adjusted resulting in improved model predictions of down gradient plumes at CHS2 and the GCREC S&GW facility. Although, no one set of parameter adjustments could capture the variability observed in the field at either site, this is not surprising based the limitations of the conceptual model.

STUMOD-FL is highly transferrable to different soil and site conditions if the limitations of the model itself are recognized and the results are interpreted appropriately. It is important to realize that STUMOD-FL-HPS was developed to be a user-friendly tool that can be used by most engineering consultants or policy makers/regulators with an engineering/science background. As a result, while the model is highly useful, it has significant limitations in modeling actual site conditions, which was intentional and necessary to meet the goals of the FOSNRS study (specifically, develop a simple to use tool). This limitation is not unique to STUMOD-FL-HPS and when a detailed modeling effort is required, the user must resort to a more complex model, such as MODFLOW/MT3D/RT3D or HYDRUS-3D. While almost any practitioner with basic knowledge of groundwater fate and transport can use STUMOD-FL-HPS, it is a much more extensive, time consuming, and expensive endeavor to implement MODFLOW-RT3D, and only expert users can accomplish the task. Moreover, such a complex modeling approach may not produce better results than the simple model (as shown by Tonsberg 2014) unless a substantial data collection campaign is performed. Even if a more complex modeling approach is chosen, the approach is highly expensive to purchase and implement and requires an extensive data set to properly calibrate/validate which generally is viewed as cost prohibitive in actual OWTS applications.

Because STUMOD-FL-HPS addresses vadose zone and groundwater flow and transport coupled with nitrogen degradation, the model is surprisingly rigorous with regard to physical and biodegradation processes given that it is designed to be a user-friendly tool. However, no simulation model is an entirely true reflection of the physical process being modeled. Thus, predictive uncertainty is required for model users to make more informed decisions. This concept was incorporated in STUMOD-FL-HPS where users can now generate cumulative frequency diagrams and make decisions based on probability rather than on point values generated by models.



## Section 5.0

### References

---

- Bradley, P.M., M. Fernandez, and F.H. Chapelle (1992). Carbon limitation of denitrification rates in an anaerobic groundwater System, *ES&T*, 26: 2377-2381.
- DeSimone, L.A. and B.L. Howes. 1998. Nitrogen transport and transformations in a shallow aquifer receiving wastewater discharge: a mass balance approach. *Water Resources Research* 34:271-285.
- Fernando, W., K. Xia, and C. Rice. 2005. Sorption and desorption of ammonium from liquid swine waste in soils. *Soil Sci Soc Am J* 69(4):1057-1065.
- Harbaugh, A. W. (2005). MODFLOW-2005, The U.S. Geological Survey Modular Ground-Water Model-the Ground-Water Flow Process, *Rep.*, 253 pp., The U.S. Geological Survey.
- Kirkland, S.L. (2001). Coupling Site-Scale Fate and Transport with Watershed-Scale Modeling to Assess the Cumulative Effects of Nutrients from Decentralized Wastewater Systems. M.S. Thesis. Dept. of Geology and Geological Engineering, Colorado School of Mines.
- Laima, M., M. Girard, F. Vouve, G. Blanchard, D. Gouveau, R. Galois, and P. Richard. 1999. Distribution of adsorbed ammonium pools in two intertidal sedimentary structures, Marennes-Oleron Bay, France. *Marine Ecology Progress Series* 182:29-35.
- Lowe, K. S., M. Tucholke, J. Tomaras, K. Conn, C. Hoppe, J. Drewes, J. McCray, J. Munakata-Marr (2009). Influent Constituent Characteristics of the Modern Waste Stream from Single Sources: Final Report. WERF, 04-DEC-1. 202 pg. PDF available at: [www.werf.org](http://www.werf.org).
- McCray, J.E., S.L. Kirkland, R.L. Siegrist, G.D. Thyne (2005). Model Parameters for Simulating Fate and Transport of On-Site Wastewater Nutrients. *Ground Water*, 43(4): 628-639.
- Parzen, R.E. (2007). Nitrogen movement and fate in a wastewater drip dispersal system in a semi-arid climate. M.S. Thesis, Environmental Science & Engineering Division, Colorado School of Mines, Golden, CO.

- Siegrist, R., R. Parzen, J. Tomaras, K. Lowe. 2014. Water movement and fate of nitrogen during drip dispersal of wastewater effluent into a semi-arid landscape. *Water Research*, 52:178-187.
- Tonsberg, C. (2014). Development of an Analytical Groundwater Contaminant Transport Model. M. S. Thesis, Civil and Environmental Engineering, Colorado School of Mines.
- Tucholke, M.B. (2007). *Statistical Assessment of Relationships Between Denitrification and Easily Measurable Soil Properties: A simple Predictive Tool for Watershed-scale Modeling*. MS Thesis, Environmental Science & Engineering, Colorado School of Mines.
- Van Raaphorst, W. and J.F.P. Malschaert. 1996. Ammonium adsorption in superficial North Sea sediments. *Continental Shelf Research* 16(11):1415-1435.
- Vogel, R.M. and A. Sankarasubramanian (2003). The validation of a watershed model without calibration, *Water Resources Research*, 39(10): 1292.
- Zheng, C., and P. P. Wang (1999). MT3DMS: A Modular Three-Dimensional Multi-species Transport Model for Simulation of Advection, Dispersion, and Chemical Reactions of Contaminants in Groundwater Systems; Documentation and User's Guide, *Contract Report SERDP-99-1 December 1999*, edited, pp. 221, U.S. Army Corps of Engineers, Washington, DC.
- Zheng, C., and G. Bennett (2002). *Applied Contaminant Transport Modeling*, 2nd ed., 621 pp., Wiley-Interscience, New York